

COLLOID TRANSPORT BY INTERFACIAL FORCES

John L. Anderson

Department of Chemical Engineering, Carnegie Mellon University,
Pittsburgh, Pennsylvania 15213

INTRODUCTION

In a historical context the interface between two phases has played only a minor role in the physics of fluid dynamics. It is of course true that boundary conditions at interfaces, usually imposed as continuity of velocity and stress, determine the velocity field of a given flow; however, this is a more or less passive use of the interface that allows one to ignore the structure of the transition between two phases. When an interface has been assigned a more active role in flow processes, it generally has been assumed that one parameter, the interfacial (surface) tension, accounts for all mechanical phenomena (Young et al. 1959, Levich & Krylov 1969). In these studies, kinematic effects of the interface were not considered, and the "no-slip" condition on the velocity at interfaces was retained. The basic message of this article is that the interface is a region of small but *finite* thickness, and that dynamical processes occurring within this region lead not only to interfacial stresses but also to an apparent "slip velocity" that, on a macroscopic length scale, appears to be a violation of the no-slip condition. The existence of a slip velocity at solid/fluid interfaces opens a class of flow problems not generally recognized by the fluid-dynamics community.

Three previous articles in this series deal with flow caused by interactions between interfaces and external fields such as electrical potential, temperature, and solute concentration. Melcher & Taylor (1969) and Levich & Krylov (1969) consider fluid/fluid interfaces where stresses produced at the interface by the external field dictate the flow. Saville (1977), on the other hand, discusses the action of an electric field on a charged solid/fluid interface and reviews the currently accepted model for electrophoretic

movement of colloidal particles. This model recognizes the diffuse nature of the charged interface and the important role of flow within the interfacial region, which leads to an apparent velocity discontinuity, or slip velocity, across the interface. The objective here is to review a class of flows generated by interactions between applied fields and solid/fluid interfaces, with electrophoresis as but one example. In order to convey this broader picture, the emphasis is on the concept of a slip velocity, the physics of its origin, and its role in determining the motion of colloidal particles.

To illustrate the importance of flow within interfacial layers, consider a small, spherical droplet suspended in a second fluid in which there is a concentration gradient of a molecular solute. If the solute affects the surface tension γ of the droplet and is insoluble within the droplet, the following expression, which was derived by Young et al. (1959),¹ gives the droplet's velocity:

$$\mathbf{U} = \frac{a}{3\bar{\eta} + 2\eta} \left(- \frac{\partial\gamma}{\partial C} \right) \nabla C_{\infty}, \quad (1)$$

where C_{∞} is the undisturbed solute concentration, a is the radius, and $\bar{\eta}$ and η are the viscosities of the interior and exterior fluids, respectively. The physical explanation of this capillary-driven phenomenon is that the solute gradient produces a gradient of tension along the droplet's surface, which drags fluid and thus propels the droplet toward regions where its surface tension would be reduced. If the droplet is solidlike ($\bar{\eta} \rightarrow \infty$), Equation (1) predicts zero velocity; however, Derjaguin et al. (1947) argued that the diffuse structure of an interface allows a finite velocity gradient through the interfacial region, which results in movement of solid particles. Recent experiments (Lin & Prieve 1983, Lechnick & Shaeiwitz 1984, Ebel et al. 1988, Staffeld & Quinn 1988a,b) demonstrate that concentration gradients of molecular solutes can, in fact, move solid particles.

The interface between two phases is a transition of finite thickness. Although the length scale of the interface may be orders of magnitude smaller than even microscopic lengths, the details of transport processes occurring within this thin layer often control the fluid dynamics outside. Electrophoresis is a good example. The charge on the particle's surface is balanced by a diffuse cloud of counterions (Figure 1). The charge density within the cloud, $\rho_c(y)$, decays exponentially in y at distances of order of the Debye screening length κ^{-1} from the surface. Taken together, the surface charge and the diffuse cloud, called the "double layer," are a neutral body; why, then, does the particle move when an electric field is

¹Young et al. actually derived the velocity of a droplet in a temperature gradient.

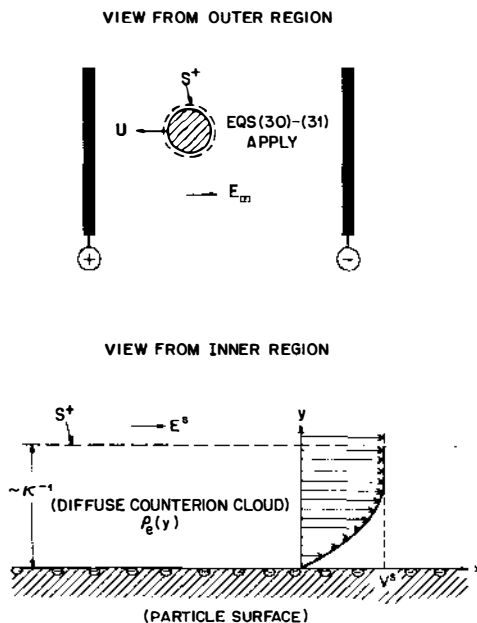


Figure 1 Electrophoresis of a charged particle. κ^{-1} is the Debye screening length of the solution, defined by (4). v^s is the "slip velocity," which is given by (6) with ζ (taken to be negative here) equal to the electrostatic potential at $y = 0$. E^s is the electric field at the outer edge of the double layer (S^+).

applied? The answer is that this neutral body is not rigid, and the diffuse cloud of counterions moves in the opposite direction of the charged particle. The velocity field within the thin layer of space charge determines the velocity field outside the layer. The fluid velocity at the outer edge S^+ of the double layer differs from the particle's velocity U by the slip velocity v^s , which results from electrically driven flow of the space charge inside S^+ as shown at the bottom of Figure 1. The length scale of the double layer is κ^{-1} . Neutrality of the particle plus counterion cloud means the applied electric field exerts zero force on the surface S^+ , and hence the velocity decays to zero as r^{-n} , where $n > 1$. These hydrodynamic characteristics cause electrophoresis and other "phoretic transport" to differ significantly from flows associated with sedimentation, where the external field exerts a net force on a particle.

Phoretic transport is defined as the movement of colloidal particles by a field that interacts with the surface of each particle; examples are listed in Table 1. By their basic nature these phenomena involve an interplay among fluid dynamics, surface science, and transport of mass, charge, and

Table 1 Transport of solid colloidal particles by phoretic processes in liquids. The slip-velocity coefficient b is defined by (31)

$U = b\nabla Y_\infty^a$			
Name	Field variable (Y_∞)	b	Remarks
Electrophoresis	Electrical potential	$\frac{\epsilon\zeta}{4\pi\eta}$	ζ = zeta potential of particle surface
Diffusiophoresis	Concentration of a chemical species (nonionic)	$\frac{kT}{\eta} KL^*$	See (11) for K and L^*
Diffusiophoresis	Concentration of a chemical species (ionic)	$4 \frac{kT}{\eta} \kappa^{-2} \left[\frac{\bar{\zeta}}{2} \beta - \ln(1 - \xi^2) \right]^b$	$\bar{\zeta} = Ze\zeta/kT$; see (4) for κ^{-1} , (13) for ξ , and (17) for β
Thermophoresis	Temperature	$y\hat{h} dy$	\hat{h} is the local specific enthalpy increment at distance y from the solid surface: $\hat{h} = h(y) - h(\infty)$

^a $Y_\infty(\mathbf{x})$ is the undisturbed field. See the assumptions leading to (34).

^b The first term inside the brackets assumes (17) for the local electric field; this is valid if (33) applies.

thermal energy. Motion of a particle is induced by an applied field $Y_{\infty}(\mathbf{x})$, which is usually electrical potential, temperature, or the concentration of a molecular solute in the fluid. Only *linear* phenomena are considered here, and hence the particle's velocity is proportional to ∇Y_{∞} . There are several distinguishing features of phoretic transport. First, the presence of the particle and any other boundary disturbs the field, and this disturbance must be computed before the Stokes-flow equations can be solved to obtain the particle's velocity. Second, there is an order-of-magnitude difference between the two important length scales, the particle's radius and the thickness of the interfacial region. Boundary-layer ideas apply naturally to the Stokes equations, with the velocity field at the outer edge of the interfacial region forming the inner boundary condition for flow in the outer fluid. Finally, a most important characteristic of phoretic transport is that the external field applies no force to the particle plus the fluid in the interfacial region; to the outer fluid the moving particle appears to be force free and torque free, and the flow about the particle decays quickly, as mentioned in the previous paragraph. The fast decay of the fluid velocity about a moving particle has important implications for the effects of fixed boundaries on phoretic transport rates, as discussed later.

The logical starting point is to examine the concept of slip velocity at *solid/fluid* interfaces by considering specific models for which the physics is reasonably understood. Mechanisms by which an electric field or gradient of solute concentration directed parallel to a planar interface causes flow within an interfacial layer are discussed in the next section. The question of whether slip velocity should be considered a material property of an interface, in the absence of a well-defined model for flow in the interfacial region, is then raised. The slip velocity is used as a prescribed boundary condition of Stokes flow in the outer fluid to obtain the velocity of a particle suspended in a gradient of electrical potential, solute concentration, or temperature. The arbitrariness of defining a particle as "fluid" or "solid" is discussed in the context of apparent discontinuities in both stress and velocity across an interface. In general, flows within the interfacial layer do not affect the fields (electrical potential, etc.) in the outer fluid, but under certain circumstances this is not true and corrections must be made for "polarization" of the interfacial region. Effects of particle interactions and fixed boundaries on particle velocity clearly show basic differences between transport by surface forces versus transport by body forces such as gravity. Recently published experimental results for particle transport are cited not only to demonstrate the existence of slip velocity but also to argue for the quantitative value of the models for slip velocity presented here. In the concluding remarks some ideas are presented about how microfields established by active processes within a particle, such as

a living cell, could self-propel the particle through a fluid. This model of locomotion illustrates a mechanism by which chemical or electrical energy could be converted to flow.

DYNAMICS WITHIN INTERFACIAL LAYERS

The concepts of “slip velocity” and “stress discontinuity” are related to the scale of view; that is, the velocity and stress are continuous on the length scale of the thickness of the interfacial region δ but appear discontinuous on the scale of the size of the particle. With fluid/fluid interfaces the apparent stress discontinuity (surface-tension gradient) controls the dynamics [see (1)], and there are many good references for flows generated by gradients of surface tension, sometimes called “Marangoni effects” or “capillary-driven flow” (Young et al. 1959, Sternling & Scriven 1959, Levich & Krylov 1969, Subramanian 1981). However, with solid/fluid interfaces the discontinuity in stress is trivial and the slip velocity controls the dynamics. In this section we focus on slip velocity and the physics behind it.

In flows involving colloidal suspensions and porous media the fluid is divided into two regions—the “inner” region comprising the interfacial layer at the surface of the particles or the pore walls, and the “outer” region including all the fluid outside the interfacial layer. The length scales of the inner and outer regions (δ and R , respectively) are generally orders of magnitude different, so that it is often possible to treat the inner region geometrically as a flat plate and apply classical boundary-layer ideas. The velocity field within the inner region is obtained first, and its value at the outer edge is used as a boundary condition for flow in the outer region. In the models for flow in the inner region that are presented below, the fluid is assumed to be Newtonian. Furthermore, all solid surfaces are assumed smooth on the length scale of the interfacial region, and inertial forces are neglected.

Electroosmosis: Flow by Electric Fields

The basic model for flow adjacent to a charged solid surface is attributed to Helmholtz (see Hiemenz 1986). As shown in Figure 1, the fixed charge on the surface (shown arbitrarily as negative in the figure) is balanced by a diffuse space charge $\rho_e(y)$ that equals the difference between the concentrations of counterions (positive here) and coions (negative). E^s is the electric field at the outer edge of the double layer; its direction defines the x -axis. This field acts on the space charge to produce a body force on the fluid equal to $\rho_e E^s$. The x -component of the Stokes equation is

$$\eta \frac{\partial^2 v_x}{\partial y^2} + \rho_e E^s = 0. \quad (2)$$

The pressure gradient parallel to the surface is negligible because of the boundary-layer approximation; that is, dp/dx is $O(R^{-1})$, where R is the length scale of the particle, and is thus negligible compared with the other two terms in the limit $\delta/R \rightarrow 0$. The charge density is related to the double-layer electrostatic potential $\Psi(y)$ by Poisson's relation

$$\rho_e = -\frac{\epsilon}{4\pi} \frac{\partial^2 \Psi}{\partial y^2}. \quad (3)$$

The length scale for the double layer is the Debye screening length, given by

$$\kappa^{-1} = \left[\frac{8\pi Z^2 e^2}{\epsilon kT} C^s \right]^{-1/2} \quad (4)$$

C^s is the electrolyte concentration at the outer edge of the double layer ($\kappa y \rightarrow \infty$), Z is the valence of the positive and negative ions of the electrolyte, e is the charge of an electron, ϵ is the fluid dielectric constant, and kT is the thermal energy. Combining (2) and (3) and integrating gives the following velocity profile:

$$v_x = \frac{\epsilon}{4\pi\eta} [\Psi(y) - \zeta] E^s, \quad (5)$$

where ζ is the so-called zeta potential, which equals Ψ at $y = 0$ (Hunter 1981). Note that the no-slip boundary condition, $v_x = 0$ at $y = 0$, was used to derive (5), and the velocity gradient at $y \rightarrow \infty$ was set equal to zero. The latter boundary condition results when the velocity field in the inner region is matched with the outer region to guarantee continuity of stress; the velocity gradient is $O(R^{-1})$ in the outer region and hence zero on the scale of the inner region. The zeta potential can be related to the surface charge through the Gouy-Chapman model for the double layer (Hiemenz 1986).

The slip velocity is defined as the value of v_x at the outer limit of the inner region:

$$v^s = \lim_{y \rightarrow \infty} v_x = -\frac{\epsilon \zeta}{4\pi\eta} E^s. \quad (6)$$

This velocity, which is directed parallel to the solid surface, is what the fluid in the outer region sees. Although the electric field E^s is determined by charge transport in the outer region, the fluid is electrically neutral and

conductive processes dominate, so that this field is usually independent of the fluid dynamics. Once E^s is calculated at every point along the solid surface, v^s is a boundary condition for Stokes flow in the outer region, as discussed in the next section. Typical values of the parameters are $|\zeta| \approx kT/e$, $E^s \approx 1 \text{ V cm}^{-1}$, $\eta \approx 0.01$ poise, and $\varepsilon \approx 78$ (water); thus, v^s is of order micrometers per second.

An important point about (6) is that E^s and ζ can be functions of position x along the interface as long as their gradients are $O(R^{-1})$. The fact that ζ can vary over the surface was only recently appreciated and was subsequently used to develop models for electrophoresis of nonuniformly charged particles (Anderson 1985a, Fair & Anderson 1988).

Osmosis: Flow by Gradients of Neutral Solutes

Uncharged solute molecules dissolved in a liquid interact with surfaces through excluded volume effects as well as dipole and van der Waals forces. The total interaction is represented by a potential energy $\Phi(y)$, called the "potential of mean force," such that $-\nabla\Phi$ is the force experienced by a molecule at distance y from the surface. This force is transmitted to the fluid and in aggregate results in a body force $-C\nabla\Phi$, where C is the local solute concentration. Since Φ has a length scale of δ , the y -variation of C is given by the equilibrium expression of Boltzmann:

$$C = C^s \exp(-\Phi/kT), \quad (7)$$

where $C^s(x)$ is the concentration at the outer edge of the inner region and varies along the surface with a gradient of $O(R^{-1})$. The momentum balances on the fluid in the y - and x -directions in the limit $\delta/R \rightarrow 0$ become

$$\frac{\partial p}{\partial y} + C \frac{d\Phi}{dy} = 0, \quad (8a)$$

$$\eta \frac{\partial^2 v_x}{\partial y^2} - \frac{\partial p}{\partial x} = 0. \quad (8b)$$

By combining (7) and (8a) one finds the pressure field; substituting this pressure into (8b) and solving for the velocity at $y \rightarrow \infty$ then gives the slip velocity:

$$v^s = -\frac{kT}{\eta} \int_0^\infty y [\exp(-\Phi/kT) - 1] dy \frac{dC^s}{dx} \quad (9)$$

The above result for v^s was originally derived by Derjaguin et al. (1947).

Figure 2 shows a hypothetical concentration profile of solute near a solid surface, with y measured on the scale of δ . The potential energy is related to the local concentration through (7). The slip velocity, given by (9), can be reexpressed in terms of two parameters of the solute profile, K and L^* (Anderson et al. 1982):

$$v^s = -\frac{kT}{\eta} KL^* \frac{dC^s}{dx}, \quad (10)$$

$$K = \int_0^\infty [\exp(-\Phi/kT) - 1] dy, \quad (11)$$

$$L^* = K^{-1} \int_0^\infty y [\exp(-\Phi/kT) - 1] dy.$$

The “adsorption length” K equals the area under the excess-concentration profile shown in Figure 2. It represents the amount of solute adsorbed, per area of surface, divided by the bulk concentration at equilibrium. The first moment of the solute distribution, L^* , is expected to be $O(\delta)$, but its precise value can only be calculated from knowledge of $\Phi(y)$; there is no method of directly measuring L^* . Although K must be positive if the solute adsorbs to the surface, L^* could be positive or negative depending on the form of the energy profile.

A model system of an adsorbing solute for which $\Phi(y)$ is calculable a

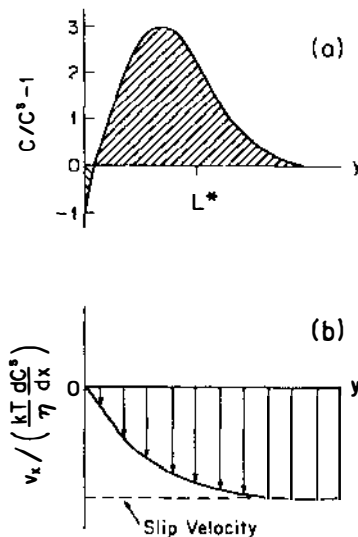


Figure 2 (a) Hypothetical excess-solute profile at a solid/liquid interface. K is the net area under the curve, while L^* is the first moment as defined by (11). (b) Velocity field relative to the fixed solid when the far-field concentration C^s varies along the surface. The slope at $y = 0$ equals $-K$.

priori is the interaction of a neutral, dipolar molecule with the electrical double layer of a charged surface (Koh & Anderson 1978). The solute's dipole moment (μ_D) aligns with the local electric field of the double layer, $E_d = -d\Psi/dy$, such that the energy is

$$\Phi = -kT[\mu^* \coth(\mu^*) - 1], \quad (12)$$

where $\mu^* = E_d \mu_D / kT$. The Gouy-Chapman theory (Hiemenz 1986) of planar double layers gives

$$E_d = (4kT/Ze)\kappa \xi \exp(-\kappa y) / [1 - \xi^2 \exp(-2\kappa y)],$$

$$\xi = \tanh\left(\frac{Ze\zeta}{4kT}\right), \quad (13)$$

where Z is the valence of the supporting electrolyte (e.g. $Z = 1$ for potassium chloride), ζ is the zeta potential of the surface, and κ is given by (4). Combining (11)–(13) produces the following result, which is correct to $O(\xi^4)$:

$$KL^* = \frac{4}{3} \left(\frac{\mu_D}{Ze}\right)^2 \xi^2 \left\{ 1 + \frac{\xi^2}{2} \left[1 + \frac{4}{5} \left(\frac{\mu_D \kappa}{Ze}\right)^2 \right] \right\}. \quad (14)$$

For small solute molecules ($MW \leq 100$), μ_D does not usually exceed 20×10^{-18} esu cm. Assuming this value for the dipole moment along with $\xi = 1/2$ ($\zeta \approx 2kT/e$) and $\kappa = 10^7 \text{ cm}^{-1}$, we have

$$KL^* = 5.8 \times 10^{-16} \text{ cm}^2.$$

If the solute concentration gradient is 0.1 mole cm^{-4} , a reasonable value in boundary layers, then substitution of the above numerical values into (10) and use of the viscosity of water at 25°C gives $v^s \approx -2 \mu\text{m s}^{-1}$, which is a fairly typical magnitude for a slip velocity.

A second example for which Φ is known is the steric (entropic) exclusion of rigid solute "particles." If the solute particles are spheres of radius a , then $\Phi \rightarrow \infty$ when $y < a$ and $\Phi = 0$ when $y > a$; use of this potential energy in (11) gives

$$KL^* = -a^2/2. \quad (15)$$

The negative sign means that v^s is directed toward *higher* solute concentration. Steric exclusion is the mechanism behind the classical view of osmosis—that is, flow from low to high osmotic pressure (Anderson & Malone 1974). Nonspherical solute particles are treated in a similar way, with $\Phi(y)$ determined by averaging the probability over all orientations

at fixed y . The following results are easily derived for extremely long solute rods and thin solute disks:

$$\begin{aligned} KL^* &= -(1/24)l^2 \quad (\text{rods, length } l), \\ &= -(1/3)c^2 \quad (\text{disks, radius } c). \end{aligned} \quad (16)$$

Osmosis: Flow by Gradients of Charged Solutes

A gradient of a strongly dissociating electrolyte produces flow within the inner region by two mechanisms. The first involves excess pressure within the double layer at the charged surface, akin to the stresses developed with neutral solutes discussed above. The second mechanism is based on the electric field that is generated in the outer region because the diffusion coefficients of the two ions are not equal. If the local current is *zero* in the outer region, the diffusion electric field is proportional to β , which is defined as $(D_+ - D_-)/(D_+ + D_-)$ for a symmetric electrolyte $M^{+z}X^{-z}$:

$$E^s = \frac{kT}{Ze} \beta \frac{d \ln C^s}{dx}. \quad (17)$$

The contributions from these two mechanisms add to give the following slip velocity (Prieve et al. 1984):

$$v^s = -\frac{\varepsilon \zeta}{4\pi\eta} E^s + \frac{\varepsilon}{2\pi\eta} \left(\frac{kT}{Ze} \right)^2 \ln(1 - \zeta^2) \frac{d \ln C^s}{dx}, \quad (18)$$

where ζ is defined in Equation (13). The second term on the right in (18) is called the ‘‘chemiphoretic’’ effect and causes flow toward *lower* electrolyte concentration, while the first term is the ‘‘electrophoretic’’ effect and causes flow in the direction determined by the sign of the product $\beta\zeta$.

Thermoosmosis: Flow by Temperature Gradients

Derjaguin et al. (1987) developed a model for the slip velocity at a solid/liquid interface resulting from a tangential temperature gradient. This theory is based on computing the flux of energy (enthalpy) carried by forced (pressure-driven) convection of fluid across a porous barrier and applying Onsager’s reciprocal theorem to obtain the momentum flux that would result from an applied temperature gradient. By equating the momentum flux to the mean flow velocity of liquid through the pores, he obtained the following expression for the slip velocity at the pore walls:

$$v^s = -\frac{2}{\eta} \int_0^\infty y \hat{h}(y) dy \frac{d \ln T^s}{dx}, \quad (19)$$

where $\hat{h}(y)$ is the local excess specific enthalpy (erg cm^{-3}) in the interfacial

layer compared with the bulk liquid. If the solid surface is *lyophilic*, meaning the liquid phase is attracted at the molecular level, then $\hat{h} < 0$ and the slip velocity is directed toward higher T^s .

The problem with (19) is that there is currently no molecular model from which to compute $\hat{h}(y)$. The surface excess enthalpy,

$$H^e = \int_0^\infty \hat{h}(y) dy, \quad (20)$$

is a measurable, macroscopic quantity similar in concept to K [see (11)]; however, the experimental determination of H^e is considerably more difficult than K . Furthermore, there is still the problem of estimating the length parameter L^* , defined here essentially the same as for diffusio-phoresis [see (11)]. Derjaguin et al. (1987) cite experimental results that demonstrate the existence of thermoosmosis in porous media.

Relation Between Slip Velocity and Stress Discontinuity at an Interface

The physical models developed above are intended to demonstrate possible origins of slip velocity. While experiments have shown their predictive capabilities to be good, as discussed later, these models are only semiquantitative, since simplifications have been introduced, such as constant viscosity and dielectric constant. In the discussion below, a more general approach is taken to support the notion of slip velocity at any interface where the interfacial energy varies. The objective is to demonstrate in a general way that the same stress distribution within an interfacial region leads to both a gradient of interfacial tension and an apparent discontinuity in fluid velocity across the interface.

The pressure tensor within an interface is anisotropic (Brenner 1979, Davis & Scriven 1982):

$$\mathbf{P} = P_N \mathbf{nn} + P_T(y) [\mathbf{I} - \mathbf{nn}], \quad (21)$$

where \mathbf{n} is the unit normal to the interface, \mathbf{I} is the unit dyadic, and y is measured along \mathbf{n} on the length scale of the interfacial thickness. A force balance normal to a flat interface shows P_N to be constant. The interfacial tension is given by

$$\gamma = \int_{-\infty}^{\infty} (P_N - P_T) dy. \quad (22)$$

The local pressure anisotropy, $P^* \equiv P_N - P_T$, depends on thermodynamic variables; if one of these (Y) varies along the interface, say in the x -direction, then a gradient of shear stress develops:

$$\frac{\partial \sigma_{yx}}{\partial y} + \frac{\partial P^*}{\partial x} = 0, \quad \frac{\partial P^*}{\partial x} = \frac{dY^s}{dx} \left(\frac{\partial P^*}{\partial Y} \right)_{Y=Y^s}, \tag{23}$$

where, as before, the superscript *s* denotes the value of *Y* at the outer edge of the interfacial region. Integration once over the entire interface gives the stress discontinuity, which is apparent on the length scale of the bulk-phase fluids:

$$\tau^s \equiv \sigma_{yx}(+\infty) - \sigma_{yx}(-\infty) = -\frac{dy}{dx}. \tag{24}$$

Levich & Krylov (1969) review the use of τ^s as a boundary condition for flow in the bulk phases.

Because at least one of the two phases bounding the interface is fluid, a nonzero shear stress must result in flow parallel to the interface. Assume that the fluid is Newtonian with a position-dependent coefficient of viscosity. The velocity field v_x is found by integrating (23) twice over y and matching the velocity gradient at $y \rightarrow \pm \infty$ with the gradients of the bulk phases. The slip velocity should be independent of the velocity gradients in the bulk phases; this is true if the ‘‘interface’’ $y = 0$ is defined such that

$$\int_{-\infty}^0 \left[\frac{1}{\eta} - \frac{1}{\eta_-} \right] dy + \int_0^{\infty} \left[\frac{1}{\eta} - \frac{1}{\eta_+} \right] dy = 0, \tag{25}$$

where η_+ and η_- are the viscosities of the bulk phases. The resulting expression for slip velocity is

$$\begin{aligned} v^s &= \lim_{y \rightarrow +\infty} \left[v_x - \left(\frac{\sigma_{yx}}{\eta_+} \right) y \right]_{y \rightarrow -\infty} \frac{-}{\eta_-} \\ &= \frac{d}{dx} \int_{-\infty}^{+\infty} \int_0^y \frac{1}{\eta} dy \int_0^{+\infty} \left[\frac{1}{\eta} \frac{1}{y} \frac{1}{\eta_+} \right] dy \end{aligned} \tag{26}$$

It is evident that v^s arises from the same intermolecular forces as τ^s —that is, the forces that produce P^* .

To connect this general result with the specific model for osmosis ($Y = C$), assume that $\eta(y)$

$$v^s = \frac{d}{dx} \left[\frac{1}{\eta_-} \int_{-\infty}^0 y P^* dy + \frac{1}{\eta_+} \int_0^{\infty} y P^* dy \right]. \tag{27}$$

If the solute concentration is sufficiently low to have a thermodynamically ideal solution, the Gibbs equation relating changes in interfacial free energy to surface excess concentration of the solute (Hiemenz 1986) can be used to show

$$\frac{d}{dx} \int_{-\infty}^{\infty} P^* dy = -kT \left[\int_{-\infty}^{y_0} \left(\frac{C}{C_-^s} \right) \frac{dC_-^s}{dx} + \int_{y_0}^{\infty} \left(\frac{C}{C_+^s} - 1 \right) dy \frac{dC_+^s}{dx} \right], \quad (28a)$$

where C_{\pm}^s is the bulk fluid concentration of solute on each side of the ‘‘Gibbs dividing surface’’ $y = y_0$, and C is the local concentration within the interfacial region. Note that C_-^s and C_+^s are related by principles of phase equilibria. The Gibbs dividing surface is close to but not exactly at $y = 0$, the surface defined by (25).² In the case of linear solute adsorption, C/C_{\pm}^s is independent of C_{\pm}^s and hence independent of x . If we assume such a condition with $y_0 = 0$, (28a) suggests that

$$P^* = -kT[C - C_{\pm}^s], \quad (28b)$$

which gives the following when substituted into (24) and (27):

$$\tau^s = kT \frac{d}{dx} \int_{-\infty}^{\infty} [C(y, x) - C_{\pm}^s(x)] dy, \quad (29a)$$

$$v^s = -kT \frac{d}{dx} \int_{-\infty}^{\infty} \frac{1}{x} \eta_{\pm} \quad - \quad (29b)$$

where the subscripts $+$ and $-$ mean that these bulk-phase values are to be inserted for $y > 0$ and $y < 0$, respectively. Thus, for osmotic flows with neutral solutes, the stress and velocity discontinuities across the interface are proportional to the zeroth and first moments of the surface excess concentration, respectively. Equation (9) is recovered from (29b) by setting $\eta_- \rightarrow \infty$ (solid) and using (7) to relate C to C_+^s .

In light of the above discussion, one can justifiably put forth the general relation

$$v^s = -b \nabla Y^s,$$

where the slip-velocity coefficient b can be considered a material property of the interface, depending only on local thermodynamic conditions. Values of b (see Table 1) can be extracted from the specific models discussed earlier, represented by Equations (6), (9), (18), and (19).

² Schofield & Henderson (1982) discuss the arbitrariness in defining the exact location of an interface.

PHORETIC TRANSPORT OF RIGID PARTICLES

When viewed on the length scale of particle size R , the actual surface of the particle and the surface S^+ that encloses the particle *plus* the interfacial region appear identical in the limit $\delta/R \rightarrow 0$. Flow in the region outside S^+ is governed by the classical Stokes equations:

$$\eta \nabla^2 \mathbf{v} - \nabla p = 0, \quad \nabla \cdot \mathbf{v} = 0, \quad (30a)$$

$$\text{on } S^+: \quad \mathbf{v} = \mathbf{U} + \boldsymbol{\Omega} \times \mathbf{r} + \mathbf{v}^s, \quad r \rightarrow \infty: \mathbf{v} \rightarrow \mathbf{0}. \quad (30b)$$

The translational and angular velocities of the particle are determined by solving the flow problem stated above, assuming \mathbf{v}^s is known at all points on the surface, with the further constraint that the *force* and *torque* exerted by the fluid on S^+ are *zero*:

$$\iint_{S^+} \mathbf{n} \cdot \boldsymbol{\sigma} dS = \mathbf{0}, \quad \iint_{S^+} \mathbf{r} \times (\boldsymbol{\sigma} \cdot \mathbf{n}) dS = \mathbf{0}, \quad (30c)$$

where $\boldsymbol{\sigma}$ is the fluid stress tensor. The reason for this constraint is that the external field Y_∞ exerts no force on the particle plus its interfacial layer. Thus, phoretic transport represents a novel fluid-dynamics problem where a force-free body moves at just the proper velocity to negate the prescribed slip velocity, which is determined by the external field.

From the previous section we see that the slip velocity \mathbf{v}^s is proportional to a gradient of a potential function Y such as voltage, solute concentration, or temperature:

$$\mathbf{v}^s = -b \nabla Y^s, \quad (31)$$

where Y^s is the limiting value of Y as S^+ is approached from the outer fluid. Values of b that were derived in the previous section are listed in Table 1.

Because the particles of interest are micron size and the velocities are generally less than $100 \mu\text{m s}^{-1}$, Peclet numbers are small in the outer fluid and Y is described by Laplace's equation:

$$\nabla^2 Y = 0, \quad (32a)$$

$$r \rightarrow \infty: \nabla Y \rightarrow \nabla Y_\infty \text{ (a constant)}, \quad (32b)$$

where Y_∞ is the undisturbed field, which is assumed linear here. If $\delta/R \rightarrow 0$, the no-flux boundary condition at the surface applies:

$$\text{on } S^+: \mathbf{n} \cdot \nabla Y = 0. \quad (33)$$

As shown later, (33) can be in error if the interfacial layer has a finite capacity to transport solute molecules; this is called a “polarization” effect.

Smoluchowski (1921) solved the above problem, (30)–(33), for the specific case of electrophoresis of a *sphere*. Smoluchowski’s result can be written in general form for any phoretic transport phenomenon described by the above equations:

$$\mathbf{U} = b\nabla Y_\infty, \quad \boldsymbol{\Omega} = \mathbf{0}. \quad (34)$$

Morrison (1970) made the important observation that the velocity field in the fluid about a sphere moving by electrophoresis is a *potential flow*:

$$\mathbf{v} = \frac{1}{2} \left(\frac{a}{r} \right)^3 \left[3 \frac{\mathbf{r}\mathbf{r}}{r^2} - \mathbf{I} \right] \cdot \mathbf{U}. \quad (35)$$

He then proved that a potential-flow solution that satisfies all the above fluid-dynamic boundary conditions can be obtained for particles of any shape. Finally, he showed that (34) holds for particles of *arbitrary shape* as long as (a) Y is described by (32)–(33), and (b) the value of b is constant over the particle’s surface. Corrections needed to account for nonconstant b or polarization effects [i.e. (33) is invalid] are discussed later in this section. It has long been assumed that Smoluchowski’s equation applies to the electrophoresis of particles of arbitrary shape when the double layer is thin, but Morrison was the first to prove the correctness of this assumption from a fluid-dynamics basis.

The potential-flow character of the velocity field about a moving particle distinguishes phoretic transport from sedimentation in a nontrivial way. The velocity disturbance is $O(r^{-3})$, compared with $O(r^{-1})$ for sedimentation. As shown later, this difference has important consequences regarding the effects of boundaries and particle interactions on phoretic transport.

General Representation for Spheres With Thin Interfacial Layers

Smoluchowski’s equation [generalized as (34)] could be in error, even when δ/R is small, for at least two reasons. First, the capacity of the interfacial layer to exchange solute molecules with the outer fluid can be finite if the solute/surface interactions are strongly attractive, a possibility recognized by Dukhin & Derjaguin (1974) in their analysis of electrophoretic processes. In this case boundary condition (33) must be altered, as discussed later. Second, the coefficient b of (31) might vary over the surface of the particle. To account for these effects, a general analysis of the Stokes-flow problem is needed to provide an easy method to compute the

translational and rotational velocities of a particle given the dependence of the slip velocity over the entire surface S^+ .

Lamb's solution to the Stokes equations provides a convenient method to solve for the velocity field about a sphere with a prescribed velocity on its surface (Brenner 1964). The following result can be derived using only (30) (Anderson & Prieve 1988):

$$\mathbf{U} = -\langle \mathbf{v}^s \rangle, \quad (36a)$$

$$\boldsymbol{\Omega} = (3/2a)\langle \mathbf{v}^s \times \mathbf{n} \rangle, \quad (36b)$$

where a is the particle's radius, \mathbf{n} is the unit normal on the surface, and the brackets denote an area average over the surface of the sphere (or, more precisely, S^+):

$$\langle g \rangle = \frac{1}{A} \int \int_{S^+} g \, dA.$$

The problem is thus reduced to solving for ∇Y^s and using (31) to represent the slip velocity at each point.

First consider a nonuniform field for which (32b) is replaced by $Y \rightarrow Y_\infty(\mathbf{x})$, where the undisturbed field Y_∞ is not necessarily linear. By solving (32a) with an arbitrary $Y_\infty(\mathbf{x})$, applying (33) at the surface, and then substituting the result into (36), one finds that (34) still holds with ∇Y_∞ evaluated at the position of the particle (Keh & Anderson 1985). This means that a sphere having uniform surface properties and negligible polarization of the interfacial region cannot be rotated simply by applying a spatially varying field. Of course, the velocity field around the moving particle differs from (35) if ∇Y_∞ is not constant; a curious result is that the velocity disturbance associated with $\nabla \nabla Y_\infty$ is $O(r^{-2})$ and hence longer range than the flow caused by ∇Y_∞ .

The case of nonuniform surface properties on a sphere can be handled by (36) as well. For a field satisfying (32)–(33), use of (31) with b an arbitrary function of position on the surface gives the following result (Anderson 1985a):

$$\mathbf{U} = \left[\langle b \rangle \mathbf{I} - \frac{1}{2} \langle (3\mathbf{nn} - \mathbf{I})b \rangle \right] \cdot \nabla Y_\infty, \quad (37a)$$

$$\boldsymbol{\Omega} = \frac{9}{4a} \langle \mathbf{nb} \rangle \times \nabla Y_\infty. \quad (37b)$$

These expressions reduce to (34) when b is constant. The dipole moment of b creates a rotation tending to align the dipole with the gradient. Sample

calculations indicate that a very small dipole moment of the zeta potential, for example, could lead to almost total alignment of a particle in an electric field. It is reasonable to expect that many colloidal particles have a distribution of charge that leads to such a dipole moment. Colloid scientists have not made an effort to detect the alignment of individual particles in electric fields, probably because there has been unfailing belief in the general applicability of (34) with ζ taken to be an area-averaged value.

Distortion of the Applied Field: Interfacial Polarization

The velocity of a spherical particle depends on the average driving force (∇Y^s) over the particle's surface, according to (31) and (36). The result (34) was derived assuming the field variable obeys (32) and (33). There are two situations where one of these equations is incorrect, as discussed below.

If the ambient fluid undergoes forced convection in a direction perpendicular to the macroscopic gradient, the field variable may not be described by the conduction equation. Convection has no effect on electrical potential because the outer fluid is electrically neutral; thus, (34) remains valid for electrophoresis. In the case of diffusiophoresis or thermophoresis, however, fluid convection distorts the concentration or temperature field about the particle, and thus (32a) must be replaced by the steady convective-diffusion equation. Convection reduces the magnitude of ∇Y^s (Leal 1973), and at very strong flows (large Peclet numbers) the gradient approaches zero everywhere along the surface (Nir & Acrivos 1976). This "micromixing" effect of laminar flow about a particle reduces the phoretic velocity (Anderson et al. 1987).

Polarization of the interfacial layer could also result from a strong attractive interaction between solute molecules and a particle's surface, thus causing (34) to be incorrect even at very small values of δ/R . This is because boundary condition (33) is derived from a simple geometric argument based on the fact that the area for transport within the interfacial layer is $O(\delta/R)$ compared with the area for diffusion from the outer fluid into the interfacial region. Dukhin (see Dukhin & Derjaguin 1974) noted that if there is strong attraction between solute molecules and the surface, then the excess solute concentration in the interfacial layer, which is $O(K/\delta)$ larger than the concentration in the outer fluid, is quite large. Therefore, the ratio of the solute transport rate within the interfacial region to the transport rate in the outer fluid is actually $O(K/R)$, which could be significant even if the interfacial layer is very thin. Dukhin's arguments are somewhat obscure; Fixman (1980) and O'Brien (1983) have reformulated these ideas in a tighter mathematical development.

The essential feature of interfacial polarization is that transport within

the interfacial region affects the distribution of chemical species in the outer fluid. In the case of diffusiophoresis caused by gradients of neutral solute molecules, (33) is replaced by

$$\text{on } S^+: \mathbf{n} \cdot \nabla Y = -\lambda \nabla_s^2 Y, \quad (38)$$

where ∇_s^2 is the two-dimensional Laplacian in the plane of the interface.³ The right-hand side is a “surface-conduction” term that results from integrating the diffusive and convective transport of solute over the thickness of the interfacial layer (Anderson & Prieve 1988). The surface conductivity λ is of order K [defined in (11)], so that the right side is $O(K/R)$ relative to the left. If (38) is used instead of (33), the velocity of a spherical particle is given by

$$\mathbf{U} = (1 + \lambda/a)^{-1} b \nabla Y_\infty. \quad (39)$$

This result, which is exact in the asymptotic limit $\delta/a \rightarrow 0$, says that for large particles \mathbf{U} is independent of particle size, while for particles smaller than λ the velocity is proportional to particle size.

For electrophoresis and diffusiophoresis in gradients of charged solutes, the analysis of polarization is more involved because conservation equations must be solved for both the electrical potential and the electrolyte concentration. O’Brien (1983) has developed a model for handling thin double layers that is based on the original work of Dukhin. O’Brien & Hunter (1981) used this model to derive an analytical expression for the electrophoretic mobility of a spherical particle, which agrees very well with the numerical solution to the electrophoretic problem (O’Brien & White 1978) over a broad range of ζ and κa . The essence of the model is the use of (38) as a boundary condition for the transport of electrolyte ($Y = C$) and charge ($Y = V$). The λ -values are calculated by integrating the diffusive and convective flux of the counterion (the ion of the electrolyte having a charge opposite in sign to the zeta potential) over the thickness of the double layer. The right side of (38) is order $(\kappa a)^{-1} \exp[Ze|\zeta|/2kT]$ compared with the left side, so that the classical boundary condition (33) does not necessarily apply if the zeta potential is too large, even if $(\kappa a)^{-1}$ is small.

A most intriguing effect of double-layer polarization was discovered by Prieve & Roman (1987) for diffusiophoresis in gradients of electrolytes for which the ion mobilities are equal ($\beta = 0$). From (17) one might infer that only the second term on the right side of (18) makes a contribution to the velocity when $\beta = 0$. It can be shown that this term (the chemiphoretic effect) always causes a slip velocity toward lower electrolyte concentration,

³ ∇_s is the projection of the gradient operator onto the surface: $\nabla_s = (\mathbf{I} - \mathbf{nn}) \cdot \nabla$.

meaning a colloidal particle should move toward higher electrolyte concentration. While this is true for small magnitudes of ζ , Prieve & Roman's numerical solution of the relevant transport equations indicates that the particle's velocity *reverses direction* at large values of ζ . An explanation for this reversal is found by realizing that (17) only applies when there is zero current; a finite E^s can develop along the particle's surface, even when $\beta = 0$, because of the capacity of the double layer to carry significant current via transport of the counterion. Since the total current must be zero, one can easily demonstrate that the induced electric field is directed such that it forces the particle in a direction opposite to the chemiphoretic effect. As the magnitude of ζ increases, the chemiphoretic contribution decreases and the electrophoretic effect increases, and a change in the direction of movement of the particle occurs.

Nonspherical Particles

From Morrison's (1970) analysis we know that (34) is a general solution to (30)–(33) for particles of any shape. The important assumptions are (a) that δ is everywhere much smaller than the local mean radius of curvature of the particle, (b) that polarization effects are negligible, and (c) that b is constant over the particle's surface. The electrophoretic behavior of *spheroids* has been modeled when the second (O'Brien & Ward 1988) or third (Fair & Anderson 1988) assumption is relaxed.

As discussed in the previous section, double-layer polarization is a significant factor in reducing the electrophoretic mobility of a particle when $(\kappa R)^{-1} \exp[Ze|\zeta|/2kT]$ is $O(1)$. With spheroids the mobility becomes anisotropic, with the two principal mobility coefficients being smaller than the Smoluchowski value and unequal. Under polarized conditions, then, the velocity of a particle is no longer collinear with the applied electric field; however, polarization causes no rotational motions, so that a particle will not align itself with the field because of these effects.

When polarization is negligible but ζ (or b) varies over the particle's surface, the dynamics are even more interesting. A dipole moment of ζ causes rotation of the particle toward alignment of the axis with the applied field. A significant quadrupole moment causes movement skew to the field at an angle dependent upon the orientation of the particle's axis. Finally, the mean electrophoretic velocity, found by ensemble averaging over all particle orientations, is not always proportional to the area-averaged value of ζ . This means that a measured zero mobility for a particle in an electric field does not necessarily imply zero net charge or potential on the particle, a conclusion that might have important consequences on how data for the electrophoretic mobility of certain minerals are interpreted. For example, kaolinite clay particles are thin disks with a different charge on the edges

(neutral or positive) than the faces (negative). Over a broad range of pH these particles have a large quadrupole moment, which could lead to an appreciable electrophoretic mobility even when the average zeta potential (and charge) over the entire surface is zero (Fair & Anderson 1988).⁴

Fluid Particles: Role of Stress Discontinuity Versus Slip Velocity

Interfacial forces acting on fluid particles cause velocities that are proportional to the size of the particle, as shown by (1), while the velocity of solid particles is essentially independent of their size as long as polarization effects are small. This fundamental difference begs an explanation, which I attempt below. Note that the distinction between “fluid” and “solid” is not very important to transport by body forces (e.g. sedimentation), since the mobility of a gas bubble is only 33% greater than that of a solid particle.

The essential point is that the fluid-dynamical boundary condition at an interface is composed of two parts, discontinuities in both stress and velocity. For a *fluid* particle, the Stokes equations must be solved inside (denoted by an overbar) and outside to satisfy the following conditions at the surface S^+ :

$$\mathbf{n} \cdot [\boldsymbol{\sigma} - \bar{\boldsymbol{\sigma}}] \cdot (\mathbf{I} - \mathbf{nn}) = \boldsymbol{\tau}^s, \quad (40a)$$

$$\mathbf{v} - \bar{\mathbf{v}} = \mathbf{v}^s, \quad (40b)$$

plus a normal-stress condition based on the Young-Laplace equation that is only important for nonspherical droplets. From the discussion of the previous section [see (29)], we have

$$\boldsymbol{\tau}^s \sim \nabla Y^s, \quad \mathbf{v}^s \sim -\frac{\delta}{\eta} \boldsymbol{\tau}^s \quad (41)$$

Since viscous stresses in the outer fluids are $O(\eta U/R)$, where R is the particle's size, the stress discontinuity caused by the applied field results in a particle velocity $\sim (R/\eta)\nabla Y_\infty$. The slip velocity, on the other hand, results in a particle velocity $\sim \mathbf{v}^s$ that is independent of R . For spherical particles of radius a , Lamb's general solution to the Stokes equations can be used in conjunction with (40) and the zero-force constraint to obtain a general formula for the particle's velocity:

⁴To generalize the analysis by Fair & Anderson (1988) to any phoretic mechanism of transport, replace $\epsilon\zeta/4\pi\eta$ by $-b$, where b is defined by (31).

$$\mathbf{U} = -\frac{3\bar{\eta}}{2\eta + 3\bar{\eta}} \langle \mathbf{v}^s \rangle + \frac{a}{2\eta + 3\bar{\eta}} \langle \boldsymbol{\tau}^s \rangle, \quad (42)$$

where, as before, the brackets denote an average over the surface area (S^+) of the particle. The above result is valid for arbitrary \mathbf{v}^s and $\boldsymbol{\tau}^s$ as long as $\mathbf{n} \cdot \mathbf{v}^s = 0$. Ruckenstein (1981) first proposed that motion of a fluid particle in a solute concentration gradient is the sum of motions caused by the Marangoni effect ($\sim \boldsymbol{\tau}^s$) and diffusiophoresis ($\sim \mathbf{v}^s$).

To illustrate the transition from fluid to solid behavior, consider diffusiophoresis of a spherical droplet in a nonelectrolyte gradient ($Y = C$) and assume that the solute has negligible solubility inside the droplet. The variation of interfacial tension is related to the excess of solute by the Gibbs relation [Hiemenz 1986; see also (7), (11), and (29a) herein], so we have

$$\boldsymbol{\tau}^s = -\nabla\gamma = kTK\nabla C^s, \quad (43)$$

assuming that there is no contamination of the interface by extraneous surface-active chemical species. The local driving force ∇C^s is found by solving (32)–(33); substitution of the result into (42) gives

$$\mathbf{U} = \left[\frac{a + 3(\bar{\eta}/\eta)L^*}{2 + 3(\bar{\eta}/\eta)} \right] \frac{kT}{\eta} K\nabla C_\infty, \quad (44)$$

where L^* is defined by (11). Because $a \gg L^*$ in general, particles for which $\bar{\eta}/\eta$ is $O(1)$ are “fluid”; their velocity is controlled by the gradient in interfacial tension. The particles become “solid” when the internal viscosity is so high that $\bar{\eta}/\eta \gg a/L^*$; in this case the slip velocity essentially determines the velocity.

BOUNDED SYSTEMS

Effects of boundaries on interfacially driven motions of particles are considerably weaker than for movement by body forces such as gravity. There are two reasons for this. First, the velocity field about an isolated particle undergoing phoretic transport decays as r^{-3} [see (35)], compared with r^{-1} for sedimentation, which means that a boundary at distance h from the particle will exert a viscous retardation of $O(h^{-3})$ on the particle. Second, the boundary affects the field variable and thus alters the driving force (∇Y^s) on the particle’s surface. This second effect is also $O(h^{-3})$, but it often *enhances* the surface gradient, thereby tending to increase the phoretic velocity. In fact, there is one case (Keh & Chen 1988) where the enhancement of the driving force is greater than the viscous retardation,

and the velocity of a particle moving parallel to a flat wall is actually *greater* when it is very near the wall than far away.

Interactions Among Particles

A rather amazing fact is that the phoretic velocity of each of a group of N solid particles in an *unbounded* fluid, all of which have the *same* slip-velocity coefficient b , is unaffected by the presence of the other particles. The velocity of each particle is given by (34) no matter what the configuration of the particles; that is, there is *no* net effect of particle interactions. The particles can be of arbitrary shape and size, as long as $\delta \ll R$ and the surface-to-surface spacing between any two particles is always much greater than δ . A proof of this statement rests on the observation that the velocity field of the fluid can be expressed as a potential flow ($\mathbf{v} = \nabla\Phi^*$). Since both Y and Φ^* must satisfy Laplace's equation in the fluid surrounding the particles, the function $G = bY + \Phi^*$ must also satisfy Laplace's equation with the following boundary conditions:

$$\begin{aligned} \text{on } S_i^+ : \quad \nabla G = \mathbf{U}_i \quad (i = 1 \rightarrow N), \\ |\mathbf{x}| \rightarrow \infty : \quad G \rightarrow b\nabla Y_\infty \cdot \mathbf{x}, \end{aligned} \quad (45)$$

where S_i^+ designates the (outer) surface of the i th particle and \mathbf{U}_i is a constant for each i . A solution for G can only be found by letting $\mathbf{U}_i = \mathbf{U} = b\nabla Y_\infty$ for *all* N particles; G then equals $b\nabla Y_\infty \cdot \mathbf{x}$ at all points in the fluid. Furthermore, none of the particles rotates.

If the slip-velocity coefficient *varies* among the particles, however, particle interactions do affect the velocity of each particle. The particle velocities are obtained by solving Laplace's equation for Y , with (33) used on the surface of each particle. The Stokes equations must then be solved allowing for the slip velocity on the surface of each particle. The translational and angular velocities of each particle are determined such that the force and torque on it are zero. The two-sphere dynamics has the following form:

$$\begin{aligned} \mathbf{U}_1 = \mathbf{M}_{11} \cdot \mathbf{U}_{10} + \mathbf{M}_{12} \cdot \mathbf{U}_{20}, \\ \mathbf{M}_{ij} = A_{ij}\mathbf{ee} + B_{ij}(\mathbf{I} - \mathbf{ee}), \end{aligned} \quad (46)$$

where $\mathbf{U}_{i0} = b_i\nabla Y_\infty$, and \mathbf{e} is the unit vector pointing along the line between the particle centers. The mobility coefficients A_{ij} and B_{ij} are functions of the center-to-center distance r and the radii of the spheres, a_1 and a_2 . Reed & Morrison (1976)⁵ numerically solved the case of two equal-size spheres

⁵ They specifically considered electrophoresis, but their results apply to general phoretic transport by setting $b_2/b_1 = \zeta_2/\zeta_1$.

for a range of a/r and b_2/b_1 . As expected, there is no effect of particle interactions when $b_2/b_1 = 1$; thus, we know that $A_{12} = 1 - A_{11}$ and $B_{12} = 1 - B_{11}$ at all separations.

The two-sphere problem can be approximately solved for arbitrary a_2/a_1 by a method of reflections (Chen & Keh 1988) that builds on knowing how an isolated particle responds to applied fields $Y(\mathbf{x})$ and $\mathbf{v}(\mathbf{x})$ (Keh & Anderson 1985). The following is correct to $O(r^{-6})$:

$$\begin{aligned} A_{11} &= 1 - \left(\frac{a_2}{r}\right)^3 - \frac{13}{2} \frac{(a_1 a_2)^3}{r^6}, & A_{12} &= 1 - A_{11}, \\ B_{11} &= 1 + \frac{1}{2} \left(\frac{a_2}{r}\right)^3 + \frac{1}{4} \frac{(a_1 a_2)^3}{r^6}, & B_{12} &= 1 - B_{11}. \end{aligned} \quad (47)$$

This approximation is in excellent agreement with the numerical calculations of Reed & Morrison (1976) when $a/r < 0.8$. The interactions are very weak compared with those between sedimenting particles (Batchelor 1976).

The above results are for solid, spherical particles propelled by a slip velocity. The form of the interaction given in (46) also describes two spherical *fluid* droplets whose motion is determined by the gradient in interfacial tension rather than the slip velocity. The velocity field about an isolated droplet is given by (35), so that hydrodynamic interactions are $O(r^{-3})$. The velocities of two spherical droplets have been determined to $O(r^{-6})$ (Anderson 1985b). The coefficients A_{ij} and B_{ij} for two gas bubbles are the same to $O(r^{-3})$ as for two solid spheres.

Single Particle Near a Fixed Boundary

Electrophoretic motion of a spherical solid particle near a flat wall has been determined approximately by using reflection techniques (Keh & Anderson 1985) and more precisely by solving the relevant equations in bipolar coordinates (Keh & Chen 1988). The results can be generalized to any phoretic motion for which the field variable is described by (32)–(33) and the slip velocity is given by (31) at all solid interfaces. The following results for movement parallel and perpendicular to the wall were obtained by a reflection technique and have an error of $O(r^{-8})$:

$$U^{(0)} = \left[1 - \frac{1}{16} \left(\frac{a}{h}\right)^3 + \frac{1}{8} \left(\frac{a}{h}\right)^5 - \frac{31}{256} \left(\frac{a}{h}\right)^6 \right] (b_p - b_w) \nabla Y_\infty, \quad (48a)$$

$$U^{(1)} = \left[1 - \frac{5}{8} \left(\frac{a}{h}\right)^3 + \frac{1}{4} \left(\frac{a}{h}\right)^5 - \frac{5}{8} \left(\frac{a}{h}\right)^6 \right] b_p \nabla Y_\infty, \quad (48b)$$

where b_p and b_w are the slip-velocity coefficients of the particle and wall, respectively, and h is the distance of the center of the particle from the wall. For the parallel-motion case, the applied field generates a uniform fluid velocity equal to $-b_w \nabla Y_\infty$ in the absence of the particle. Note that in deriving (48a), we assumed that the wall was nonconducting ($\mathbf{n} \cdot \nabla Y = 0$), whereas in deriving (48b) we considered the wall to be a perfect conductor ($Y = 0$); the latter condition corresponds to migration of charged particles to an electrode surface. Also, (48a) applies to spheres that are free to rotate. Numerical calculations of $U^{(L)}$ over a broad range of a/h were published by Morrison & Stukel (1970).

The calculations of Keh & Chen (1988) for $U^{(II)}$ were carried to values of a/h as large as 0.995, with the important assumption that $h - a \gg \delta$. These calculations, shown in Figure 3, are in good agreement with (48a) when $a/h < 0.7$; however, at closer distances $U^{(II)}$ goes through a *minimum* and then increases as $a/h \rightarrow 1$, such that the particle moves *faster* than it would at $h \rightarrow \infty$. For example, at $a/h = 0.995$ the velocity of a freely rotating sphere is 23% *greater* than if it were far from the wall. An explanation of this enhancement of the velocity is that the driving force on the particle's surface (∇Y^s) is increased enough in the thin gap region to more than compensate for the larger viscous drag of the wall. A second

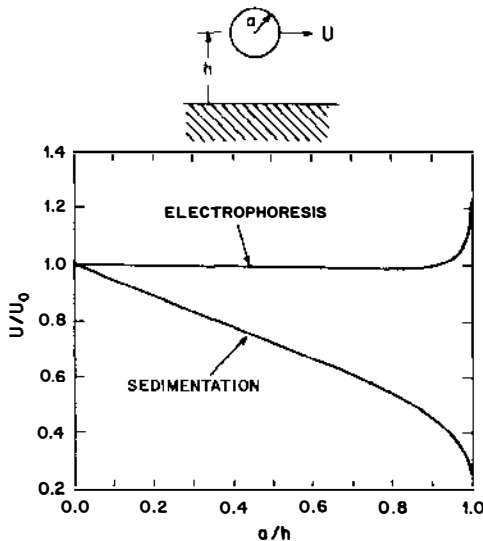


Figure 3 Wall effects on sedimentation and electrophoresis (Keh & Chen 1988) of a freely rotating sphere. The "electrophoresis" curve applies to all phenomena listed in Table 1 as long as $h - a \gg \delta$, where δ is the thickness of the interfacial region (κ^{-1} for electrophoresis).

interesting trend of Keh & Chen's calculations is that the particle's velocity is *greater* if rotation of the particle is prohibited, opposite to the behavior of a sphere undergoing sedimentation near a flat wall.

Because the effect of a fixed boundary on phoretic motion is so weak, one can imagine that a very thin fluid gap between a particle and a wall could "guide" the particle along a two-dimensional surface. Lubrication forces would stabilize the position (h) relative to the wall, while the particle remains relatively free to move in two dimensions by, say, an electric field applied parallel to the wall. This concept might apply to explaining the directed transport of colloidal-sized particles (vesicles) along fibrils extending throughout the interior of biological cells (Allen 1987, Miller et al. 1987).

The hindrance to phoretic motion experienced by a solid sphere on the centerline between two parallel plates or in a long circular tube has been determined to $O(\lambda^6)$, where λ is the ratio of the particle radius to the half-separation between the plates or the tube radius (Keh & Anderson 1985). For transport in a circular tube, we have

$$U_z = [1 - 1.2899\lambda^3 + 1.8963\lambda^3 - 1.0278\lambda^6](h_p - b_w) \frac{dY_{sc}}{dz} \tag{49}$$

with an error of $O(\lambda^8)$. The term in brackets is plotted in Figure 4 along

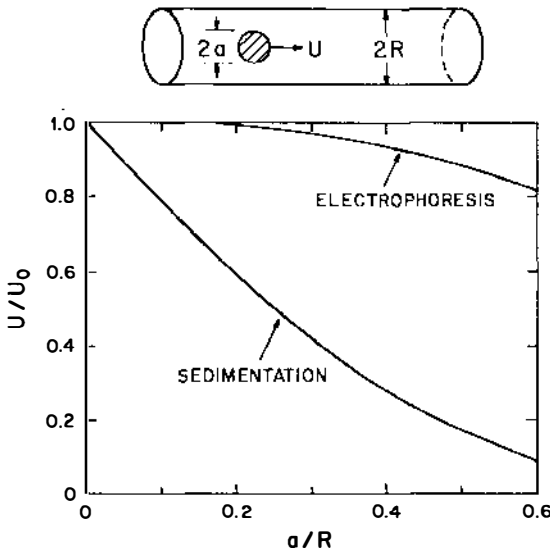


Figure 4 Sedimentation and electrophoresis of a sphere on the centerline of a long circular tube. The sedimentation results were taken from Happel & Brenner (1973). The "electrophoresis" curve applies to all phenomena listed in Table 1 and was computed from (49).

with the hindrance to movement by sedimentation. Clearly the wall effect is much weaker for the phoretic motion.

Thermocapillary transport of a spherical gas bubble near a flat wall has been studied by Meyyappan et al. (1981) for motion perpendicular to the wall and by Meyyappan & Subramanian (1987) for parallel motion. The dominant driving force for *clean* bubbles is the gradient of surface tension resulting from a nonuniform temperature field. The Peclet (or, equivalently, Marangoni) number is assumed small, so that when it is far from the wall the bubble moves at a velocity given by (1), with C replaced by T and $\bar{\eta}$ set equal to zero. The wall effect, reported as the ratio $U(h)/U(\infty)$, is determined numerically for $a/h < 0.957$ and found to be much weaker than for gravity-driven motion of the bubble. As expected, the lowest order wall effect is h^{-3} .

EXPERIMENTAL STUDIES

The electrophoretic mobility, defined as the particle velocity divided by the electric field, has stood as the most basic characterization of the charged state of a colloidal system, especially one for which water is the suspending fluid. Experimental problems associated with natural convection and non-uniform electric fields have been overcome (Hunter 1981). Smoluchowski's Equation (34) has been the accepted model for converting measured mobilities into zeta potentials (see Table 1 for b); however, experimentalists have recently become aware of the limitations of this equation at high zeta potential and now use the more precise theory embodied in the calculations of O'Brien & White (1978), which are well approximated by the formula derived by O'Brien & Hunter (1981).

Even though the number of publications reporting electrophoretic measurements on colloids is probably in the thousands, there has been little systematic and careful experimental study designed to evaluate the validity of the conventional electrokinetic theory (i.e. transport within the double layer). Zukoski & Saville (1985) measured both the electrophoretic mobility of latex particles at $C_p \rightarrow 0$, where C_p is the particle concentration, and $O(C_p)$ effects on the electrical conductance of suspensions of the particles. Extraordinary efforts were made to clean the particles and eliminate contamination that would alter the surface properties of the particles. At given conditions of pH and electrolyte concentration, each of these two measurements can be related to the zeta potential of the particles through the conventional electrokinetic theory; thus, by comparing the zeta potentials deduced from each experiment, the veracity of the theory is tested. In many cases Zukoski & Saville found good agreement, but there are some serious discrepancies that cannot be rationalized by experimental uncer-

ainties. These apparent inconsistencies have spurred the development of corrections to the theory, such as allowing for “surface conduction” of ions adsorbed on the particle’s surface.

Although the quantitative precision of the conventional theory of electrokinetics may be questioned for the colloidal latex system, there is no doubt that electric fields move charged colloidal particles and that velocity gradients within the double layer are typically $\kappa U \approx 10^3 \text{ s}^{-1}$. General acceptance, or even appreciation, of diffusiophoresis and thermophoresis is far less because very few experiments have been performed. A problem with experimentally studying diffusiophoresis is that it is difficult to establish and maintain the steep concentration gradients needed to produce velocities on the order of micrometers per second. Such gradients occur in boundary layers, for example, at the surface of a rotating disk, but the thinness of these boundary layers and the presence of a solid boundary make determination of particle velocities ambiguous. The deleterious effects of natural convection also cause problems. Anderson & Prieve (1984) review the literature dealing with experimental observations of diffusiophoresis.

Lin & Prieve (1983) were among the first to demonstrate significant diffusiophoretic transport. Their experimental method involved measurement of deposition rates of latex particles onto a porous membrane when the membrane separated a latex suspension from an electrolyte solution. The electrolyte concentration gradient extended into the latex side of the membrane through the diffusional mass-transfer boundary layer. The pores were sufficiently small to prevent the particles from passing through the membrane, so any particles that were transported through the electrolyte boundary layer deposited onto a film. The growth rate of this film, which was a measure of the particle velocity in the boundary layer, correlated very well with the measured diffusion-induced electric field [see (17)].

Another method for determining diffusiophoretic transport rates utilizes a thin porous barrier (membrane) to separate solutions differing in solute concentration. The pores should be small to stabilize the fluid against convection but large enough to allow the particles to pass unhindered. By measuring the flux of particles across the membrane under conditions of large Peclet numbers, one can determine the diffusiophoretic velocity at known values of the concentration and the concentration gradient of the solute. Lechnick & Shaeiwitz (1984) used the membrane-flux technique to measure the transport rate of latex particles in response to gradients of electrolyte solutes. Two types of experiments were performed; in one set the particle concentration was initially the same on both sides of the membrane, while in the other set there was a particle-concentration gradi-

ent at the onset. Both experiments gave clear evidence of diffusiophoresis, but for various reasons the experimental results cannot be quantitatively compared with theory.

Using the membrane technique, Ebel et al. (1988) made quantitatively accurate determinations of diffusiophoretic velocities of $0.1\text{-}\mu\text{m}$ -diameter latex spheres in electrolyte gradients. In one set of experiments they were able to generate a rather large difference in particle concentration across the membrane from an initially *uniform* particle system. In the other experiments, where initially there was a particle-concentration difference, their measurements of particle fluxes were converted to diffusiophoretic velocities and then compared with the theory without any adjustable parameters. As shown in Figure 5, the data demonstrate the predicted linearity between U and ∇C_e for fixed electrolyte concentration (C_e), and the experimental and theoretical predictions of velocity are in good agreement.

A novel apparatus to study diffusiophoresis is the stopped-flow cell developed by Staffeld & Quinn (1988a,b). A sharp boundary between solutions that differ in solute concentration is formed using a stagnation flow, as shown in Figure 6. Both solutions have the same concentration of colloidal particles. When the flow stops, the solute gradient dissipates by molecular diffusion, so that the diffusiophoretic velocity of the particles is time dependent. A band of particle-rich fluid forms on the side of the interface to which the particles are transported, and a depleted zone forms on the other side. With electrolyte gradients, Staffeld & Quinn (1988a)

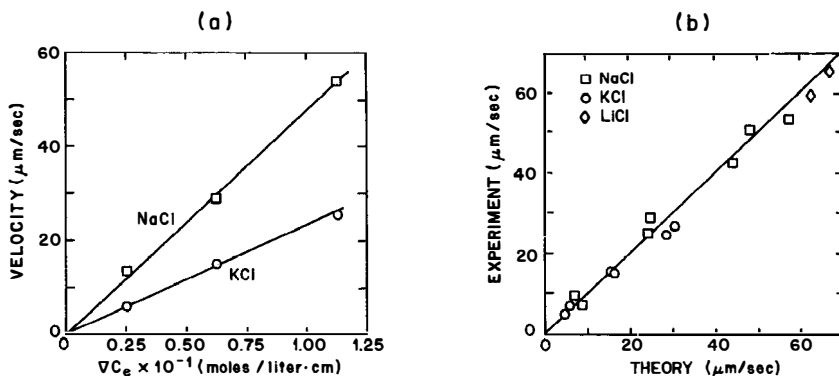


Figure 5 Diffusiophoresis experiments of Ebel et al. (1988) with $0.1\text{-}\mu\text{m}$ -diameter latex particles. (a) Measured diffusiophoretic velocity versus electrolyte gradient. C_e was fixed at 10^{-2} mol liter $^{-1}$ for all the data. (b) Experimental versus predicted values of particle velocity. The predictions were made a priori from theory (Prieve et al. 1984, Pricvc & Roman 1987) using independently measured values of ζ .

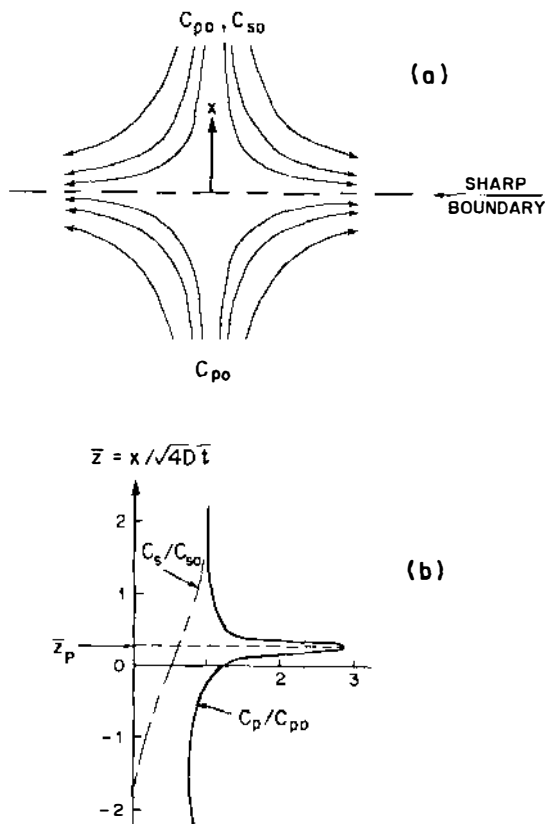


Figure 6 Diffusiophoretic experiments of Staffield & Quinn (1988a,b). (a) Planar stagnation flow was used to establish a sharp boundary between two solutions having identical particle concentrations C_{p0} but different solute concentrations (here shown as C_{s0} in the top fluid and zero in the bottom fluid). (b) After the flow is stopped, diffusiophoresis couples with diffusion to form a particle-rich band at dimensionless position \bar{z}_p , which remains constant as the solute gradient dissipates by molecular diffusion. D is the solute diffusion coefficient. The curve for C_p / C_{p0} was drawn for a condition where the diffusiophoretic velocity is toward higher solute concentration ($b > 0$).

found that the position x_p of the peak of the particle-rich band moved away from the initial boundary between the two solutions as the square-root of time, as predicted from a differential material balance on the particles that allows for both diffusion and diffusiophoresis. The theory shows that the slope of x_p versus $t^{1/2}$ depends on the coefficient relating the diffusiophoretic velocity to the local solute gradient. The experimental values of this slope for electrolyte gradients agree with predictions of

diffusiophoretic velocities based on theory (Prieve et al. 1984, Prieve & Roman 1987).

Staffeld & Quinn (1988b) also studied diffusiophoresis of micron-size latex particles in gradients of small silica spheres and polymers (dextran). For the silica gradient, the dominant solute/particle interactions were of the hard-sphere type, so that the coefficient b should be given by (15) and Table 1. As expected, the colloidal particles formed a band on the *solute-poor* side of the interface. The diffusiophoretic velocities extracted from the time dependence of movement of the particle band are in good agreement with predictions based on (15), with the effective silica radius a equal to the actual radius plus a small correction of $O(\kappa^{-1})$, where κ^{-1} is the Debye screening length of the solution. Diffusiophoresis of the particles in dextran gradients also showed movement toward lower solute concentrations; however, there is currently no theory relating KL^* to the molecular size of flexible polymers.

These experiments by Staffeld & Quinn (1988a,b) represent the first observations of diffusiophoresis in gradients of nonelectrolytes. However, the solute/particle interactions were repulsive in their system, which caused transport toward lower solute concentration. The search is still on for experimental data for diffusiophoresis in systems where the solute is strongly attracted to the particle. According to (11), such attraction could result in significantly larger velocities than in the case of repulsive interactions because the adsorption coefficient K might be orders of magnitude larger than the length scale L^* over which the interaction occurs. Derjaguin et al. (1972) observed osmotic flows across porous membranes caused by concentration gradients of molecular solutes that adsorbed to the pore walls. The direction of flow in these osmotic experiments was from high to low solute concentration, which is equivalent to suspended particles moving toward higher solute concentration. Unfortunately, the osmotic flows were weak, and quantitative interpretation of the data in terms of a model for the slip velocity, such as (10), was not feasible.

Experimental studies of thermophoresis of colloidal particles suspended in *gases* are numerous (see citations in Goren 1977, Rosner 1980) and generally show transport in the direction of colder regions. The theory of gas-phase thermophoresis is based on kinetic theory, which predicts that momentum exchanged upon collisions between gas molecules and the particle's surface drives the transport. As Derjaguin et al. (1987) argue, however, the mechanism for thermophoresis in *liquids* is not the same as in gases. This is because the liquid state is dominated by configurational effects of the molecules—that is, intermolecular potential energies—rather than by kinetic exchange of momentum. Thus, the concept of collisions between single molecules and a surface is inappropriate for solid/liquid interfaces.

McNab & Meisen (1973) measured effects of vertical temperature gradients on the sedimentation rate of micron-size, polystyrene-latex spheres in liquid water and hexane. The thermal gradient was oriented to maintain a stable density gradient in the liquid in order to avoid natural convection. The thermophoretic velocity U_t was determined by subtracting the sedimentation rate measured at zero temperature gradient from the rate measured at a finite temperature gradient. For each liquid, U_t was found to be proportional to ∇T_∞ and directed toward colder regions (downward), which shows that the slip velocity given by (19) is directed toward higher temperature. Two particle sizes were used, 0.79 and 1.01 μm diameter; the thermophoretic velocity was the same for both, prompting McNab & Meisen to conclude that thermophoresis in liquids is independent of particle size, as one would expect if the transport is caused by a slip-velocity phenomenon. Although McNab & Meisen were aware that the theory for gas-phase thermophoresis does not apply to the liquid state, they still correlated their data in a form used for gas-phase systems. In terms of my nomenclature based on (31), their data can be summarized in the form

$$b = -\frac{\alpha\nu}{T_\infty}, \quad (50)$$

where ν is the kinematic viscosity of the liquid at the ambient temperature T_∞ . (Note that my α is not the same as the α defined by McNab & Meisen.) Correlation of (50) with the thermophoresis data for both particles and both liquids gives $\alpha = 0.13$, which is about a factor of 6 less than the coefficient predicted from the theory for gases. There is no theoretical reason for α being the same for both liquids.

Experimental studies of boundary or particle-particle effects are sparse, but three such studies indicate the basic correctness of the theory. Zukoski & Saville (1987) measured the electrophoretic mobility of concentrated suspensions of red-blood-cell "ghosts" (i.e. cells that were lysed to remove the contents and then "fixed" chemically to form a more or less rigid sphere several micrometers in diameter). The measurements were made by following one "tracer" particle that was identical in size, shape, and surface properties to the other particles. Data were obtained up to particle volume fractions as high as 80%; apparently there was some deformation of the cells at these higher volume fractions. For any one population of cells, the data of Zukoski & Saville are described by the following equation:

$$U = U_0(1 - k\phi), \quad (51)$$

where ϕ is the volume fraction of particles. The empirical constant k is in the range 0.97–1.12. There should be no net interaction for a group of spheres of the same zeta potential in an unbounded fluid [see (45) and the

surrounding discussion]; thus, a statistically homogeneous suspension of spheres is slowed only by the average displacement velocity of the suspending fluid, and from hydrodynamic considerations only we expect $k = 1$ (Anderson 1981). However, one might expect the mean electric field in a bounded suspension of nonconducting particles to be affected by the particles. The fact that Zukoski & Saville determined k to be close to unity implies that the influence of the particles on the average electric field is negligible. A rigorous theoretical explanation for this result is still sought.

In their measurements of diffusiophoretic velocities of particles in electrolyte gradients, Ebel et al. (1988) observed a dependence of the velocity on pore size that is expected from the weak dependence predicted by (49). The transport rate is the product of the available area within the pore times the mean diffusiophoretic velocity. At the highest electrolyte concentrations studied, a condition when $\kappa a \approx 50$, the first-order pore-size effect determined from the experiments is consistent with a pure excluded-volume restriction on the transport area and *negligible* effect on the particle velocity inside the pore. While these experiments support the predictions of weak boundary effects on phoretic transport, there is a clear need for further experiments that directly measure the velocity of a particle inside a tube (pore) or near a fixed wall.

Differences between wall effects on gravity-driven transport of bubbles versus thermocapillary transport are demonstrated in the experiments by Merritt & Subramanian (1988). The velocity of a single gas bubble moving perpendicular (downward) to a hot plate was measured as a function of distance h from the plate. As the bubble moved toward higher temperatures, its radius a increased significantly and was measured at each position at which the velocity was determined. The measured bubble velocity was essentially constant as h decreased. In an unbounded fluid, gravitational forces would tend to move the bubble upward at a velocity $\sim a^2$, whereas thermocapillary forces force the bubble downward at a velocity $\sim a$. The fact that the measured net velocity of the bubble was *constant* as the bubble approached the plate and a was *increasing* shows that the retardation of gravity-driven motion was much greater than the retardation of thermocapillary motion. Merritt & Subramanian were able to quantitatively fit their data with theoretical calculations of wall effects on thermocapillary and gravity-driven transport, with the former being $O(h^{-3})$ and the latter $O(h^{-1})$.

CONCLUDING REMARKS

It is important to recognize that phoretic transport of solid particles can be fully understood only by considering the fluid dynamics within the

interfacial region at a particle's surface. While a thermodynamic analysis may be appealing because of its apparent simplicity, thermodynamic principles by themselves will not allow determination of the magnitude of phoretic velocities or the dependence on physical properties. In fact, the belief that a particle will spontaneously move to fluid regions where its *own* chemical potential is lower is not always correct, because spontaneity only requires that the free energy of the *total* system be lowered.

Two examples of cases where minimization of free energy of the particles leads to erroneous predictions of the *direction* of motion can be cited. The first is diffusiophoresis in gradients of electrolytes where the anion and cation mobilities are equal (Prieve & Roman 1987). At large zeta potentials, the direction of particle movement changes sign and the particle moves toward lower electrolyte concentration where, at equilibrium conditions, its chemical potential is increased. The second example is diffusiophoresis in gradients of neutral solutes when K is positive but L^* is negative [see (11)], a situation that could arise when there is a potential-energy barrier to adsorption of the solute to the particle's surface. In both of these cases, a proper analysis of free-energy changes of the entire system (particle plus solvent plus solute) is difficult because only a single particle is considered or, equivalently, the particle concentration is taken to be very small. Dissipation of the solute gradient by molecular diffusion represents a source of energy that could, in principle, drive the particle in either direction; only by solving the local conservation equations for mass, charge, and momentum transport, which in themselves represent a minimization of local free energy, can one determine the magnitude and direction of the particle's motion.

A third example of particles moving opposite to their apparent free-energy driving force is found in the experiments of McNab & Meisen (1973) on thermophoresis of solid particles in liquids. Interfacial free energies are generally decreasing functions of temperature, so that particles could lower their surface energy by moving toward hotter regions of a fluid, as bubbles and drops do (Young et al. 1959); however, McNab & Meisen observed thermal transport toward *colder* regions. It is apparent that limited insight into phoretic transport processes can be gained by merely looking at the interfacial free energy of solid particles and its dependence on macroscopic field variables.

In addition to being important to colloid science and technologies associated with the colloidal state, phoretic transport processes may also be important in certain phenomena in biological systems (Anderson 1986). Self-locomotion (chemotaxis) of single biological cells not possessing flagella (Waterbury et al. 1985) or of groups of cells (Bonner 1983) is still not understood from a mechanics viewpoint. The directed motion of vesicles

within cells (Allen 1987), which is an extremely important biological transport process, has yet to be explained. What is certain about living cells is that chemical energy is used to transport mass, charge, and momentum. A more or less straightforward application of the ideas of this paper would propose that the motility of biological particles is the result of a macroscopic field acting on their surfaces. While this is certainly a possibility, the sensitivity of biological motility to very small gradients of chemical species suggests that a more creative use of phoretic transport principles is needed.

Because living cells have internal mechanisms to convert one form of energy to another, one could envision that a small gradient of a chemical species outside a cell activates processes inside that cause the cell to create a local, microscopic gradient of a property (say, electrical potential) that propels the cell. For example, consider the hypothetical case of a spherical cell that, when it senses a gradient of a certain chemical species outside (∇C_∞), moves ions across its membrane. The current density across the membrane, from inside to outside the cell, can be expressed as

$$\text{on } S^+: j_r = \chi \mathbf{n} \cdot \nabla C_\infty, \quad (52)$$

where χ is a constant, and \mathbf{n} is the unit normal on the external surface S^+ of the cell membrane. Integration of the current density over the surface area gives a zero net exchange of charge, thus maintaining electroneutrality of the cell's interior. The conduction equation can be solved for the electrical potential in the outer fluid, given (52) as a boundary condition. The resulting electric field has a component tangent to the surface, which is given by

$$\text{on } S^+: \mathbf{E}^s = -\frac{\chi}{2k_e} (\mathbf{l} - \mathbf{nn}) \cdot \nabla C_\infty, \quad (53)$$

where k_e is the specific electrical conductivity of the outer fluid. After substituting this field into the vectorial equivalent of (6) and then using (36a) one finds that the cell moves at a velocity given by

$$\mathbf{U} = -\frac{1}{3} \left(\frac{e\zeta}{4\pi\eta} \right) \frac{\chi}{k_e} \nabla C_\infty, \quad (54)$$

where ζ is the zeta potential of the outer surface of the membrane. This simple example illustrates how active processes in a "living" particle could use the energy in a chemical gradient to propel the particle by self-electrophoresis. Numerous other examples of varying complexity could be envisioned to model locomotion. What is intriguing about such an approach is not that it describes any specific natural phenomenon, but

rather that it brings together concepts of fluid dynamics, surface chemistry, and biology in ways not considered in traditional analyses.

The focus of this paper is on transport caused by a slip velocity directed parallel to a solid surface. It is possible to have a \mathbf{v}^s that is directed *normal* to the surface; this might occur if the surface were a semipermeable membrane that allows the solvent to pass through in response to differences in osmotic pressure Π . Obviously the interior of the particle must be fluid. The membranous surface creates a no-slip condition on the *tangential* component of the fluid velocity. In this case (36) still applies, but now (31) is replaced by

$$\text{on } S^+: \mathbf{v}^s = L_p(\Pi^s - \langle \Pi^s \rangle) \mathbf{n}, \quad (55)$$

where Π^s is the local osmotic pressure at the outer surface, the brackets denote the average over the surface area, and L_p is a permeability coefficient. The osmotic pressure depends on the concentration of a molecular solute that cannot pass through the membrane; at low solute concentrations, we have $\Pi = kTC$. If C is described by (32)–(33), then (36) and (55) give the velocity of a spherical particle (called a “vesicle”) of radius a :

$$\mathbf{U} = -\frac{aL_p}{2} \nabla \Pi_\infty. \quad (56)$$

Such movement by osmotic forces is called “osmophoresis” (Anderson 1983). The velocity field outside the vesicle is irrotational and has the following form in a stationary reference frame:

$$\mathbf{v} = (a/r^3) \left[\mathbf{1} - 3 \frac{\mathbf{r}\mathbf{r}}{r^2} \right] \cdot \mathbf{U}. \quad (57)$$

Fluid is sucked into the forward hemisphere by osmotic forces and ejected across the rear hemisphere. Note that the velocity is independent of the viscosity (η) of the external fluid. The reason for this is that the motion is controlled by \mathbf{v}^s , which is determined by L_p . However, if η is comparable to a/L_p , which is $O(10^5)$ poise or greater for lipid bilayer membranes and $a \approx 1 \mu\text{m}$, then (56) is incorrect and \mathbf{U} depends on η^{-1} .

A final reminder of the differences between phoretic motions and sedimentation is provided by Figure 7. In both types of phoretic transport the velocity is $O(r^{-3})$, compared with the leading term of $O(r^{-1})$ for sedimentation. This visualization makes obvious the fact that particle/particle and particle/wall interactions are so different among these transport phenomena.

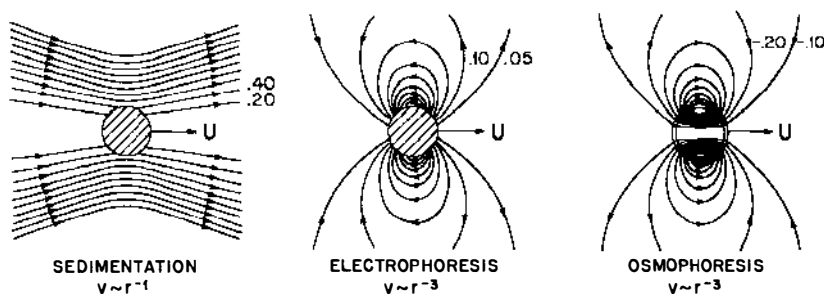


Figure 7 Streamlines for spherical particles moving by different transport mechanisms. The streamlines for "electrophoresis" are the same for any of the phenomena listed in Table 1. The numerical values on the streamlines are based on unit values of U and a . The r -dependence of the far-field velocity is given at the bottom of each drawing.

ACKNOWLEDGMENT

This work was supported by the National Science Foundation through grant CBT8513673. I appreciate very much the helpful discussions with Myung Jhon, Dennis Prieve, John Quinn, Eli Ruckenstein, and Shankar Subramanian.

Literature Cited

- Allen, R. D. 1987. The microtubule as an intracellular engine. *Sci. Am.* 265(2): 42-49
- Anderson, J. L. 1981. Concentration dependence of electrophoretic mobility. *J. Colloid Interface Sci.* 82: 248-50
- Anderson, J. L. 1983. Movement of a semi-permeable vesicle through an osmotic gradient. *Phys. Fluids* 26: 2871-79
- Anderson, J. L. 1985a. Effect of nonuniform zeta potential on particle movement in electric fields. *J. Colloid Interface Sci.* 105: 45-54
- Anderson, J. L. 1985b. Droplet interactions in thermocapillary motion. *Int. J. Multiphase Flow* 11: 813-24
- Anderson, J. L. 1986. Transport mechanisms of biological colloids. *Ann. NY Acad. Sci.* 469: 166-77
- Anderson, J. L., Malone, D. M. 1974. Mechanism of osmotic flow in porous membranes. *Biophys. J.* 14: 957-82
- Anderson, J. L., Prieve, D. C. 1984. Diffusiophoresis: migration of colloidal particles in gradients of solute concentration. *Sep. Purif. Meth.* 13: 67-103
- Anderson, J. L., Prieve, D. C. 1988. Diffusiophoresis in gradients of strongly adsorbing solutes. Submitted for publication
- Anderson, J. L., Lowell, M. E., Prieve, D. C. 1982. Motion of a particle generated by chemical gradients. Part I. Non-electrolytes. *J. Fluid Mech.* 117: 107-21
- Anderson, J. L., Prieve, D. C., Ebel, J. P. 1987. Chemically induced migration of particles across streamlines. *Chem. Eng. Commun.* 55: 211-24
- Batchelor, G. K. 1976. Brownian diffusion of particles with hydrodynamic interaction. *J. Fluid Mech.* 74: 1-29
- Bonner, J. T. 1983. Chemical signals of social amoebae. *Sci. Am.* 248(4): 114-20
- Brenner, H. 1964. The Stokes resistance of a slightly deformed sphere. *Chem. Eng. Sci.* 19: 519-39
- Brenner, H. 1979. A micromechanical derivation of the differential equation of interfacial statics. *J. Colloid Interface Sci.* 68: 422-39
- Chen, S. B., Keh, H. J. 1988. Electrophoresis in a dilute dispersion of colloidal spheres. Submitted for publication
- Davis, H. T., Scriven, L. E. 1982. Stress and structure in fluid interfaces. *Adv. Chem. Phys.* 49: 357-454
- Derjaguin, B. V., Sidorenkov, G. P., Zubashchenkov, E. A., Kiseleva, E. V. 1947. Kinetic phenomena in boundary films of liquids. *Kolloidn. Zh.* 9: 335-47
- Derjaguin, B. V., Dukhin, S. S., Koptelova,

- M. M. 1972. Capillary osmosis through porous partitions and properties of boundary layers of solutions. *J. Colloid Interface Sci.* 38: 584-95
- Derjaguin, B. V., Churaev, N. V., Muller, V. M. 1987. *Surface Forces*. New York: Consultants Bureau (Plenum). 440 pp. (Engl. transl.)
- Dukhin, S. S., Derjaguin, B. V. 1974. In *Surface and Colloid Science*, ed. E. Matijevic, Vol. 7, Chap. 3. New York: Wiley. 365 pp.
- Ebel, J. P., Anderson, J. L., Prieve, D. C. 1988. Diffusiophoresis of latex particles in electrolyte gradients. *Langmuir* 4: 396-406
- Fair, M. C., Anderson, J. L. 1988. Electrophoretic mobility of nonuniformly charged ellipsoidal particles. *J. Colloid Interface Sci.* In press
- Fixman, M. 1980. Charged macromolecules in external fields. I. The sphere. *J. Chem. Phys.* 72: 5177-86
- Goren, S. L. 1977. Thermophoresis of aerosol particles in the laminar boundary layer on a flat plate. *J. Colloid Interface Sci.* 61: 77-85
- Happel, J., Brenner, H. 1973. *Low Reynolds Number Hydrodynamics*. Leyden, Neth: Noordhoff. 553 pp.
- Hiemenz, P. C. 1986. *Principles of Colloid and Surface Chemistry*. New York: Marcel Dekker. 815 pp. 2nd ed.
- Hunter, R. J. 1981. *Zeta Potential in Colloid Science*. New York: Academic. 386 pp.
- Keh, H. J., Anderson, J. L. 1985. Boundary effects on electrophoretic motion of colloidal spheres. *J. Fluid Mech.* 153: 417-39
- Keh, H. J., Chen, S. B. 1988. Electrophoresis of a colloidal sphere parallel to a dielectric plane. *J. Fluid Mech.* In press
- Koh, W. H., Anderson, J. L. 1978. Diffusion of neutral molecules in charged pores. *J. Colloid Interface Sci.* 64: 57-67
- Leal, L. G. 1973. On the effective conductivity of a dilute suspension of spherical drops in the limit of low particle Peclet number. *Chem. Eng. Commun.* 1: 21-31
- Lechnick, W. J., Shaeiwitz, J. A. 1984. Measurement of diffusiophoresis in liquids. *J. Colloid Interface Sci.* 102: 71-87
- Levich, V. G., Krylov, V. S. 1969. Surface-tension-driven phenomena. *Ann. Rev. Fluid Mech.* 1: 293-316
- Lin, M. M. J., Prieve, D. C. 1983. Electromigration of latex induced by a salt gradient. *J. Colloid Interface Sci.* 95: 327-39
- McNab, G. S., Meisen, A. 1973. Thermophoresis in liquids. *J. Colloid Interface Sci.* 44: 339-46
- Melcher, J. R., Taylor, G. I. 1969. Electrohydrodynamics: a review of the role of interfacial shear stresses. *Ann. Rev. Fluid Mech.* 1: 111-46
- Merritt, R. M., Subramanian, R. S. 1988. Migration of a gas bubble normal to a plane horizontal surface in a vertical temperature gradient. Submitted for publication
- Meyyappan, M., Subramanian, R. S. 1987. Thermocapillary migration of a gas bubble in an arbitrary direction with respect to a plane surface. *J. Colloid Interface Sci.* 115: 206-19
- Meyyappan, M., Wilcox, W. R., Subramanian, R. S. 1981. Thermocapillary migration of a bubble normal to a plane surface. *J. Colloid Interface Sci.* 83: 199-208
- Miller, R. H., Lasek, R. J., Katz, M. J. 1987. Preferred microtubules for vesicle transport in lobster axons. *Science* 235: 220-22
- Morrison, F. A. Jr. 1970. Electrophoresis of a particle of arbitrary shape. *J. Colloid Interface Sci.* 34: 210-14
- Morrison, F. A. Jr., Stukel, J. J. 1970. Electrophoresis of an insulating sphere normal to a conducting plane. *J. Colloid Interface Sci.* 33: 88-93
- Nir, A., Acrivos, A. 1976. The effective thermal conductivity of sheared suspensions. *J. Fluid Mech.* 78: 33-48
- O'Brien, R. W. 1983. The solution of the electrokinetic equations for colloidal particles with thin double layers. *J. Colloid Interface Sci.* 92: 204-16
- O'Brien, R. W., Hunter, R. J. 1981. The electrophoretic mobility of large colloidal particles. *Can. J. Chem.* 59: 1878-87
- O'Brien, R. W., Ward, D. N. 1988. The electrophoresis of a spheroid with a thin double layer. *J. Colloid Interface Sci.* 121: 402-13
- O'Brien, R. W., White, L. R. 1978. Electrophoretic mobility of a spherical colloidal particle. *J. Chem. Soc. Faraday Trans. 2* 74: 1607-26
- Prieve, D. C., Roman, R. 1987. Diffusiophoresis of a rigid sphere through a viscous electrolyte solution. *J. Chem. Soc. Faraday Trans. 2* 83: 1287-1306
- Prieve, D. C., Anderson, J. L., Ebel, J. P., Lowell, M. E. 1984. Motion of a particle generated by chemical gradients. Part 2. Electrolytes. *J. Fluid Mech.* 148: 247-69
- Reed, L. D., Morrison, F. A. Jr. 1976. Hydrodynamic interactions in electrophoresis. *J. Colloid Interface Sci.* 54: 117-33
- Rosner, D. E. 1980. Thermal (Soret) diffusion effects on interfacial mass transport rates. *PhysicoChem. Hydrodyn.* 1: 159-85
- Ruckenstein, E. 1981. Can phoretic trans-

- port be treated as interfacial tension gradient driven phenomena? *J. Colloid Interface Sci.* 83: 77-81
- Saville, D. A. 1977. Electrokinetic effects with small particles. *Ann. Rev. Fluid Mech.* 9: 321-37
- Schofield, P., Henderson, J. R. 1982. Statistical mechanics of inhomogeneous fluids. *Proc. R. Soc. London Ser. A* 379: 231-46
- Smoluchowski, M. 1921. In *Handbuch der Elektrizität und des Magnetismus*, ed. L. Graetz, II: 366-428. Leipzig: J. A. Barth. 772 pp.
- Staffeld, P. O., Quinn, J. A. 1988a. Diffusion-induced banding of colloid particles via diffusiophoresis. Part I: Electrolytes: Submitted for publication
- Staffeld, P. O., Quinn, J. A. 1988b. Diffusion-induced banding of colloid particles via diffusiophoresis. Part II: Non-electrolytes. Submitted for publication
- Sternling, C. V., Scriven, L. E. 1959. Interfacial turbulence: hydrodynamic instability and the Marangoni effect. *AIChE J.* 5: 514-23
- Subramanian, R. S. 1981. Slow migration of a gas bubble in a thermal gradient. *AIChE J.* 27: 646-54
- Waterbury, J. B., Willey, J. M., Franks, D. G., Valois, F. W., Watson, S. W. 1985. A cyanobacterium capable of swimming motility. *Science* 230: 74-76
- Young, N. O., Goldstein, J. S., Block, M. J. 1959. The motion of bubbles in a vertical temperature gradient. *J. Fluid Mech.* 6: 350-56
- Zukoski, C. F. IV, Saville, D. A. 1985. An experimental test of electrokinetic theory using measurements of electrophoretic mobility and electrical conductivity. *J. Colloid Interface Sci.* 107: 322-33
- Zukoski, C. F. IV, Saville, D. A. 1987. Electrokinetic properties of particles in concentrated suspensions. *J. Colloid Interface Sci.* 115: 422-36